Electronic Supplementary Information for

Visualising membrane viscosity of porcine eye lens cells using molecular rotors

Peter S. Sherin,[a,b*] Ismael López-Duarte,[c] Michael R. Dent,[c] Markéta Kubánková,[c] Aurimas Vyšniauskas,[c] James A. Bull,[c] Evdokiya S. Reshetnikova,[d] Andrey S. Klymchenko,[e] Yuri P. Tsentalovich[a,b] and Marina K. Kuimova[c*]

[a] *International Tomography Center of Siberian Branch of Russian Academy of Science, Institutskaya street 3A, 630090, Novosibirsk, Russia.*
[b] *Department of Natural Sciences, Novosibirsk State University, Pirogova street 2, 630090, Novosibirsk, Russia.*
[c] *Department of Chemistry, Imperial College London, Exhibition Road, London, SW7 2AZ, UK.*
[d] *Institute of Molecular and Cellular Biology of Siberian Branch of Russian Academy of Science, 8/2 Lavrentiev Avenue, 630090, Novosibirsk, Russia.*
[e] *Laboratoire de Biophotonique et Pharmacologie, UMR 7213 CNRS, Faculté de Pharmacie, Université de Strasbourg, 74 Route du Rhin, 67401 ILLKIRCH Cedex, France.*

*E-mails: petr.sherin@tomo.nsc.ru; m.kuimova@imperial.ac.uk

Table of Content

1. Figures and Tables

1.1 Spectroscopic characterisation

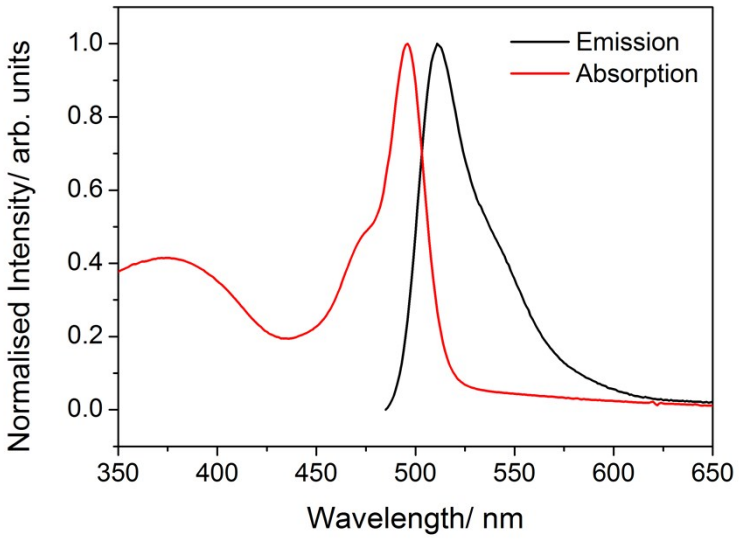

Fig. S1. Absorption and fluorescence spectra of **1c** in methanol.

It was previously established for BODIPY rotors, including **1a** and **1b**, that their fluorescence characteristics (fluorescence quantum yield and fluorescence lifetime) are temperature independent and respond to the viscosity of their environment only.[1-4] Likewise, we have demonstrated that polarity does not play a significant role in the photophysics of **1a**, at least at viscosities exceeding 30-50 cP.[3]

We have tested that our new molecular rotor **1c** responds to the viscosity of its environment rather than the temperature or the methanol/glycerol composition, by recording the time resolved fluorescence decays in mixtures of methanol/glycerol, at variable temperature (Fig. 1B, main text and Fig. S2). The data shows good overlap on the unified viscosity calibration curve, suggesting that the fluorescence lifetime of **1c** does not change as a function of temperature as already previously demonstrated for **1a, b**.[1,2,4]

From this data we conclude that **1c** responds to the viscosity of the membrane environment only, and is not affected by the measurement temperature.

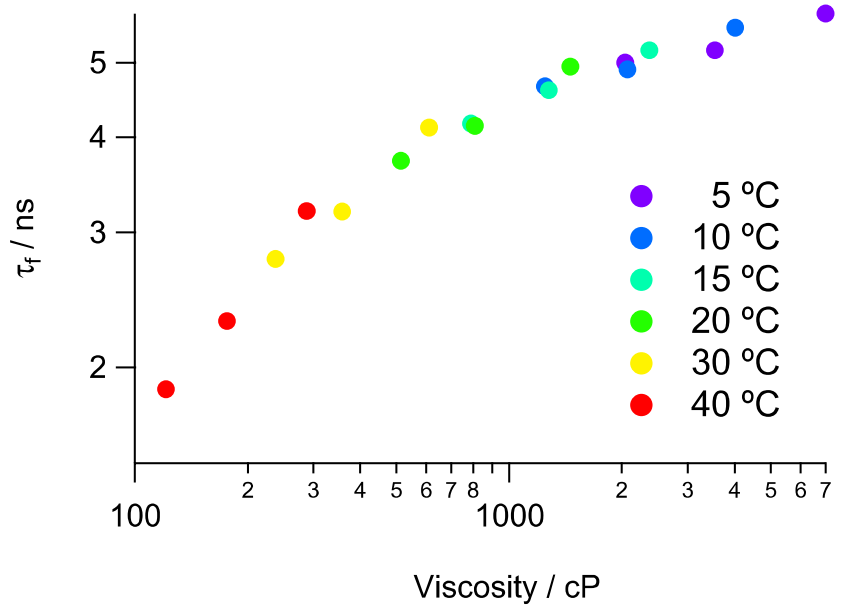

Fig. S2. Calibration of fluorescence lifetime of **1c** vs viscosity obtained in methanol/glycerol mixtures at various temperatures.

The viscosity dependence of **1c** fluorescence lifetime could be fitted by a variant of Hill function, Eq. (1) derived in our previous works:[2,5]

$$\tau = \frac{1}{a_1 \eta^{a2} + a_3} \quad (1),$$

where η is viscosity and a_i are fitting parameters. The best fit of data, presented in Fig. 1B of the main text, were obtained with parameter values $a_1 = 0.0241$, $a_2 = -0.872$, $a_3 = 1.65 \times 10^{-4}$ and presented as red curve in Fig. S3.

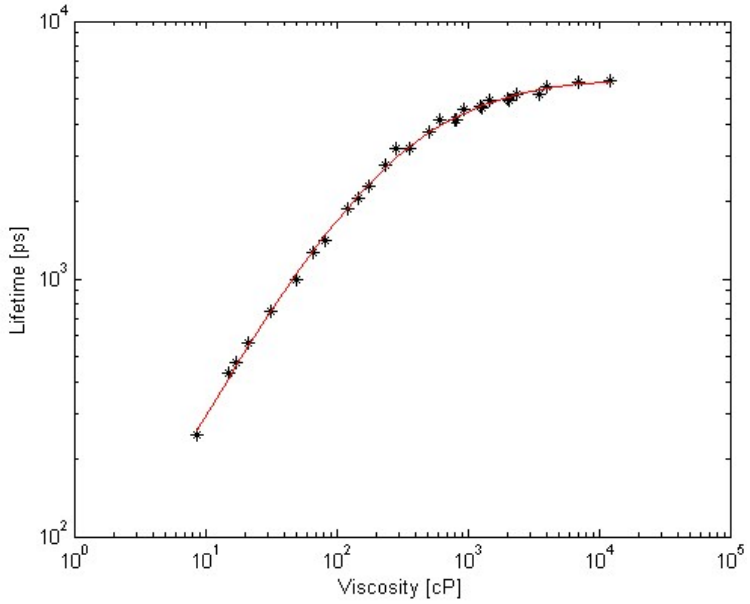

Fig. S3. Fitting of the lifetime calibration data for **1c** according to equation (1).

1.2 Imaging

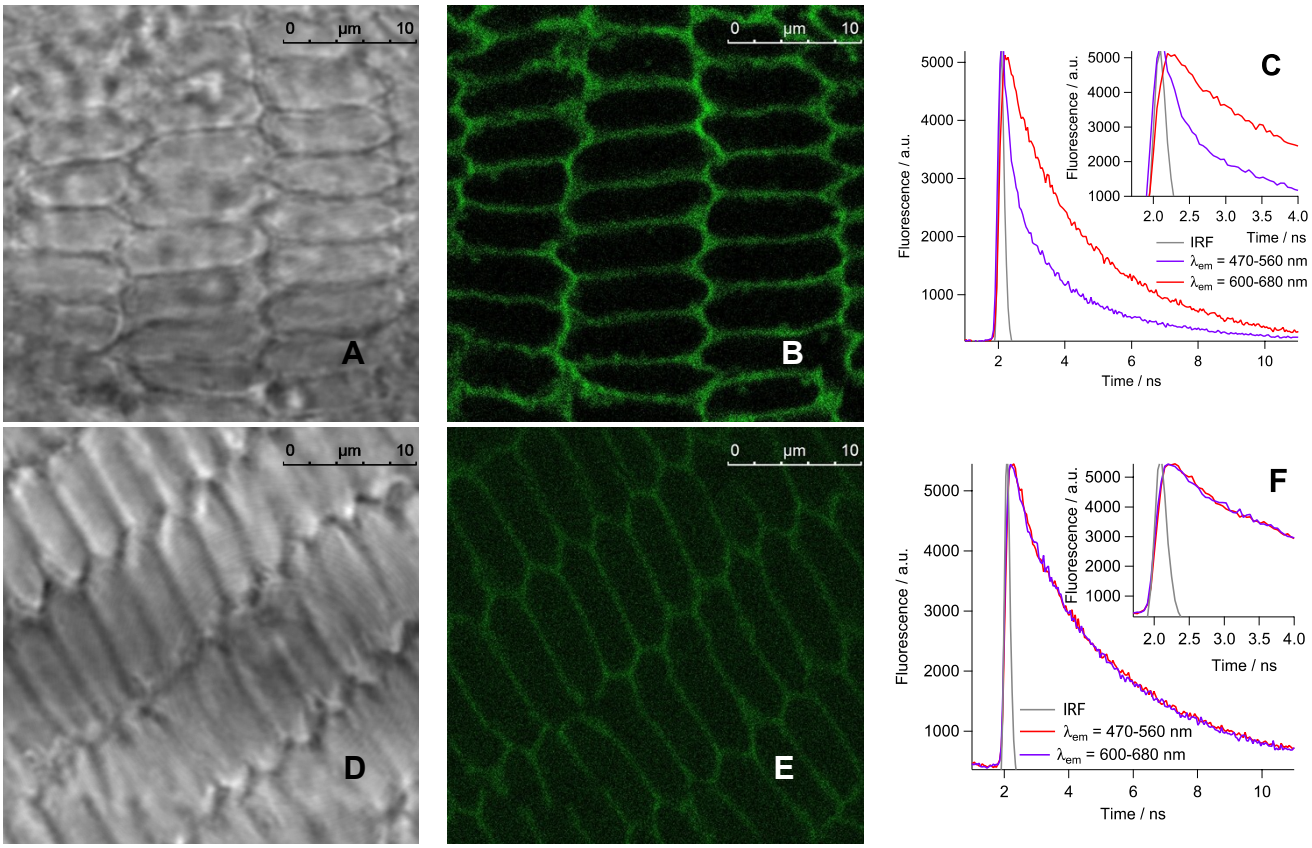

Fig. S4. (A, D) Transmission and (B, E) confocal images and (C, F) fluorescence time profiles recorded for porcine eye lens slices stained with 10 µM solutions of (A, B, C) **1a** and (D, E, F) **1b** in PBS. (C, F) Time profiles were recorded following two-photon excitation at 920 nm and detection in two spectral ranges 470-560 and 600-680 nm. Insets: zoom into the early-time dynamics of the same data.

It is well known that for BODIPY-based dyes the presence of a biexponential decay can be a hallmark of dye aggregation.[1] The aggregated species are characterised by a weak emission band centered at 650-700 nm, which can be difficult to detect spectrally. Upon aggregation the quenching of the main emission band centered at 515 nm is observed,[1] which renders the lifetime-viscosity calibration curve unusable. It follows that the comparison between time resolved decays recorded at 470-560 nm and at 600-680 nm should confirm the presence of aggregated species, should the decay be different at these two wavelength ranges (with more significant contribution from a long lifetime component typical of aggregated species observed at > 600 nm).

It is easy to see that **1a** shows strong evidence for aggregation in lens cell membranes (Fig. S4C) while the decays recorded for **1b** and **1c** in the two spectral windows described above are identical (Fig. S4F and S6). At the same time it is also clear that the staining of the lens cell membranes with **1b** was inefficient, with binning of 7x7 achieving only 300 counts in the decay maximum (on average across the image).

The staining with **1c** was **considerably** more efficient and we detected no evidence of aggregation of **1c**, even when the measurements were repeated at increasing concentrations of **1c** (1, 3 and 10 µM, Fig. S6). This data confirms that the biexponential decays of **1c** are not due to the presence of aggregates but rather indicate the fact that the rotor can probe the microscopic heterogeneities in the lens membranes. Based on the previous modeling and experimental data for **1a-b**[3] we assign the biexponential decay of **1c** to two different localisations in the lipid membrane: in the lipid tail region (long lifetime, *ca.* 50 % amplitude) and in the head region of lipids (short lifetime, *ca.* 50 % amplitude).

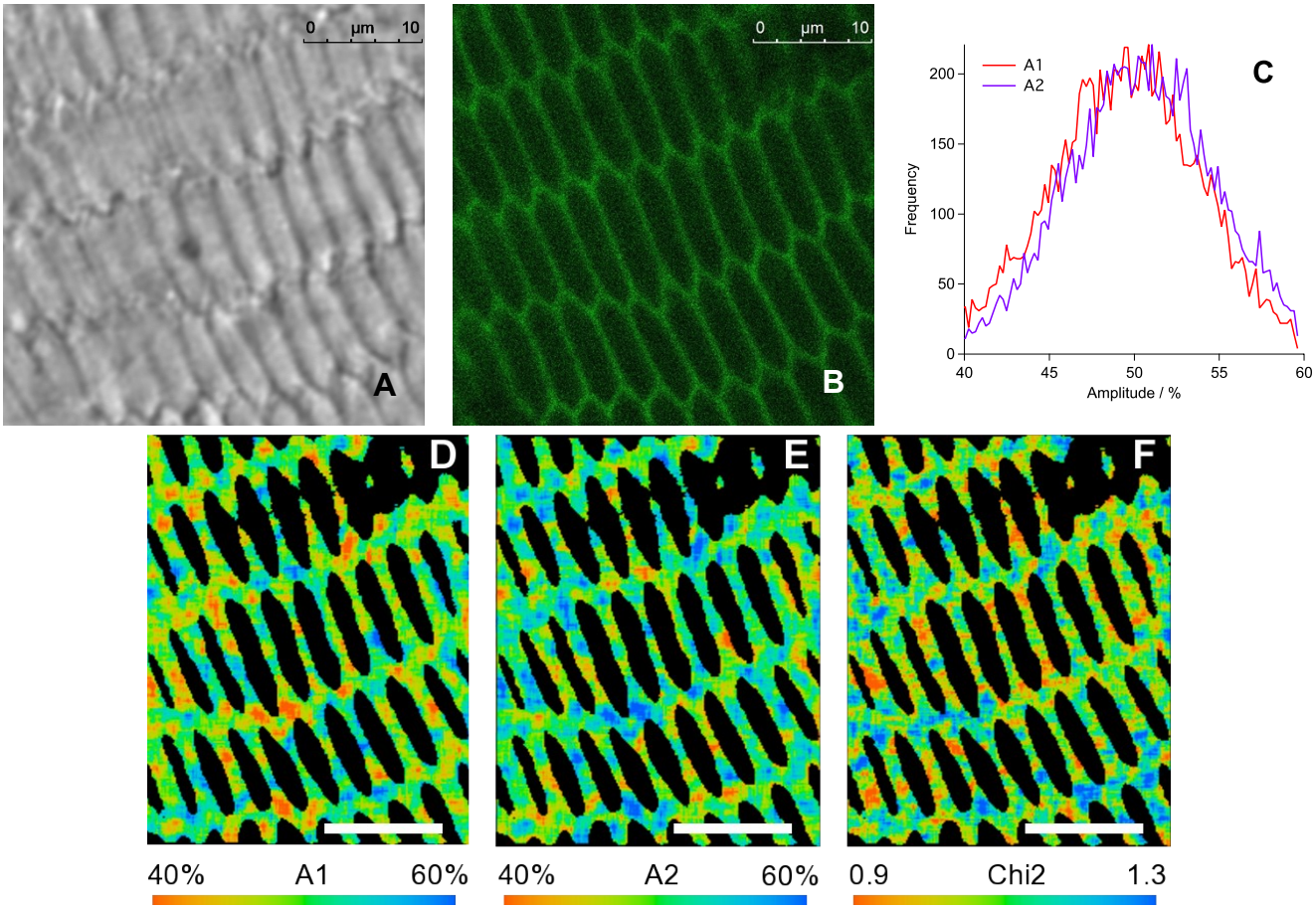

Fig. S5. Confocal and FLIM images of porcine eye lens slices stained with 10 µM PBS solution of **1c**. (A) Confocal transmittance image 35x35 µm; (B) confocal fluorescence image 35x35 µm: excitation at 476 nm and emission in the range of 490-560 nm; (C) histograms of amplitudes, A_1 and A_2, obtained from the biexponential analysis of FLIM data, 920 nm excitation, 470-560 nm detection; (D-F) pseudo-color maps of (D) A_1, (E) A_2 and (F) χ^2 goodness of fit distributions. Scale bar = 10 µm.

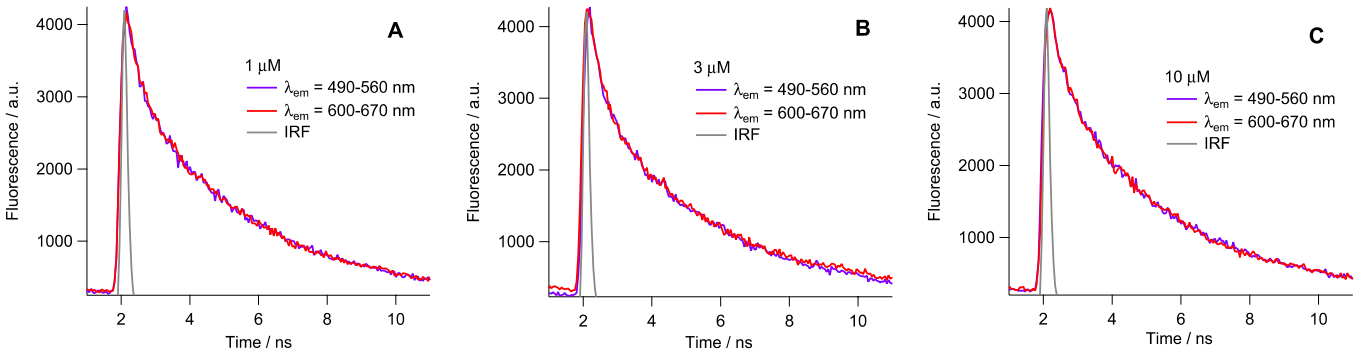

Fig. S6. Time-resolved fluorescence decays recorded from porcine eye lens slices stained with different concentrations of **1c** (1, 3 and 10 µM) in PBS following two photon excitation at 920 nm and detection in two spectral ranges 480-560 nm (monomers) and 600-670 nm (aggregates).

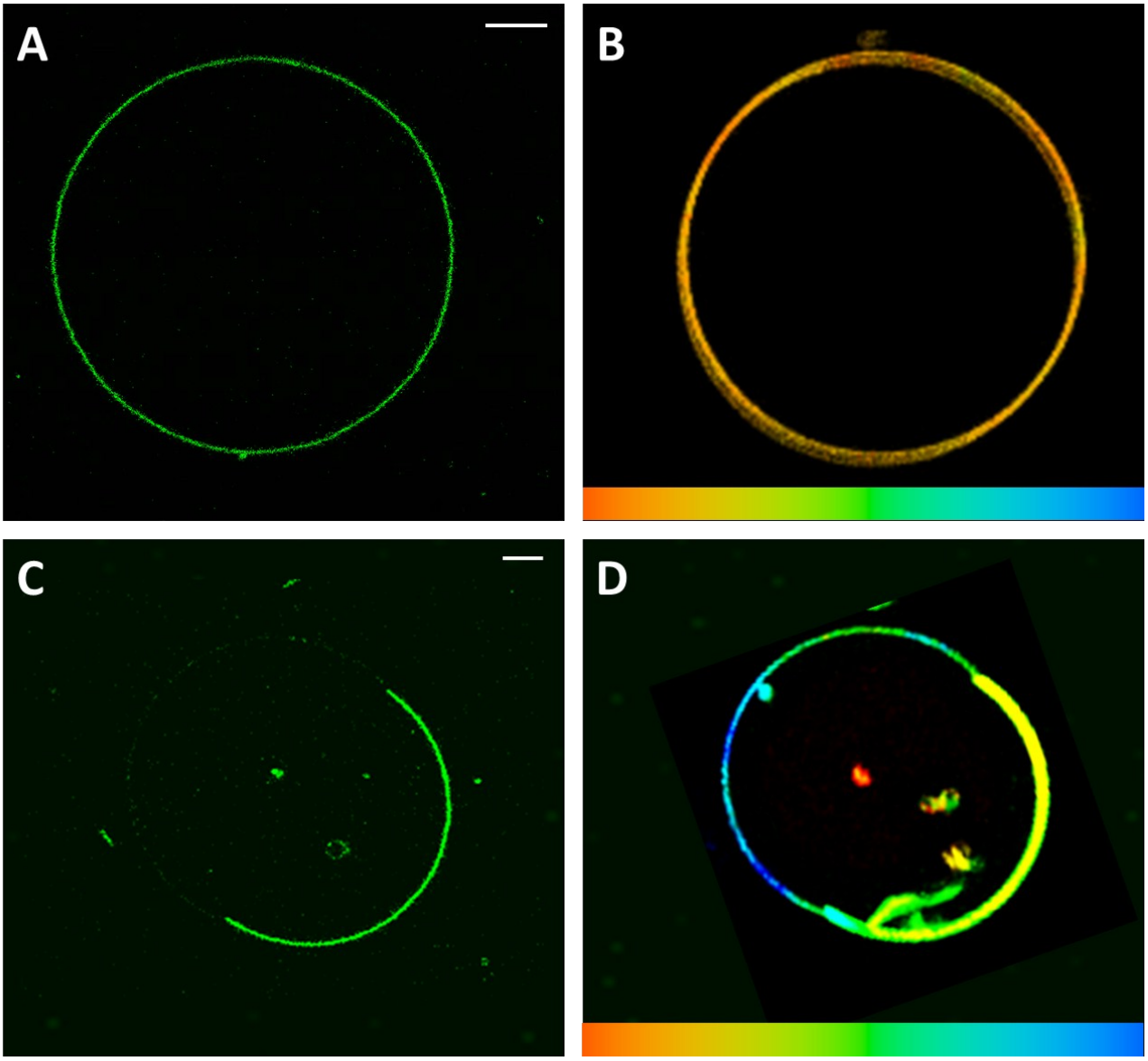

Fig. S7. (A, C) Confocal and (B, D) FLIM images of **1c** in pure DOPC (A, B) and phase separated GUVs (20:55:25 DOPC:EYSM:cholesterol) (C, D). **1c** was incorporated at 1:200 [dye]:[lipid] to avoid aggregation effects.

We have confirmed that **1c** incorporates into all model membranes, at various lipid compositions, although the staining of the liquid ordered (L_o) phase was *ca.* ten times weaker compared to the liquid disordered (L_d) phase in a ternary 20:55:25 1,2-dioleoyl-sn-glycero-3-phophocholine (DOPC): egg yolk sphingomyelin (EYSM) : cholesterol phase separated system, Fig. S7C. This is consistent with data for other previously investigated BODIPY rotors.[3]

It could be seen that the fast decay component, < 0.2 ns, is present in all decays (< 10 % in DOPC and 40-60% of the decay in EYSM) which is equivalent to the lifetime of **1c** in an aqueous environment. By analogy with previously reported data for **1b**[3] we assign this fast component to a small fraction of the dye residing in an aqueous phase, outside the bilayer.

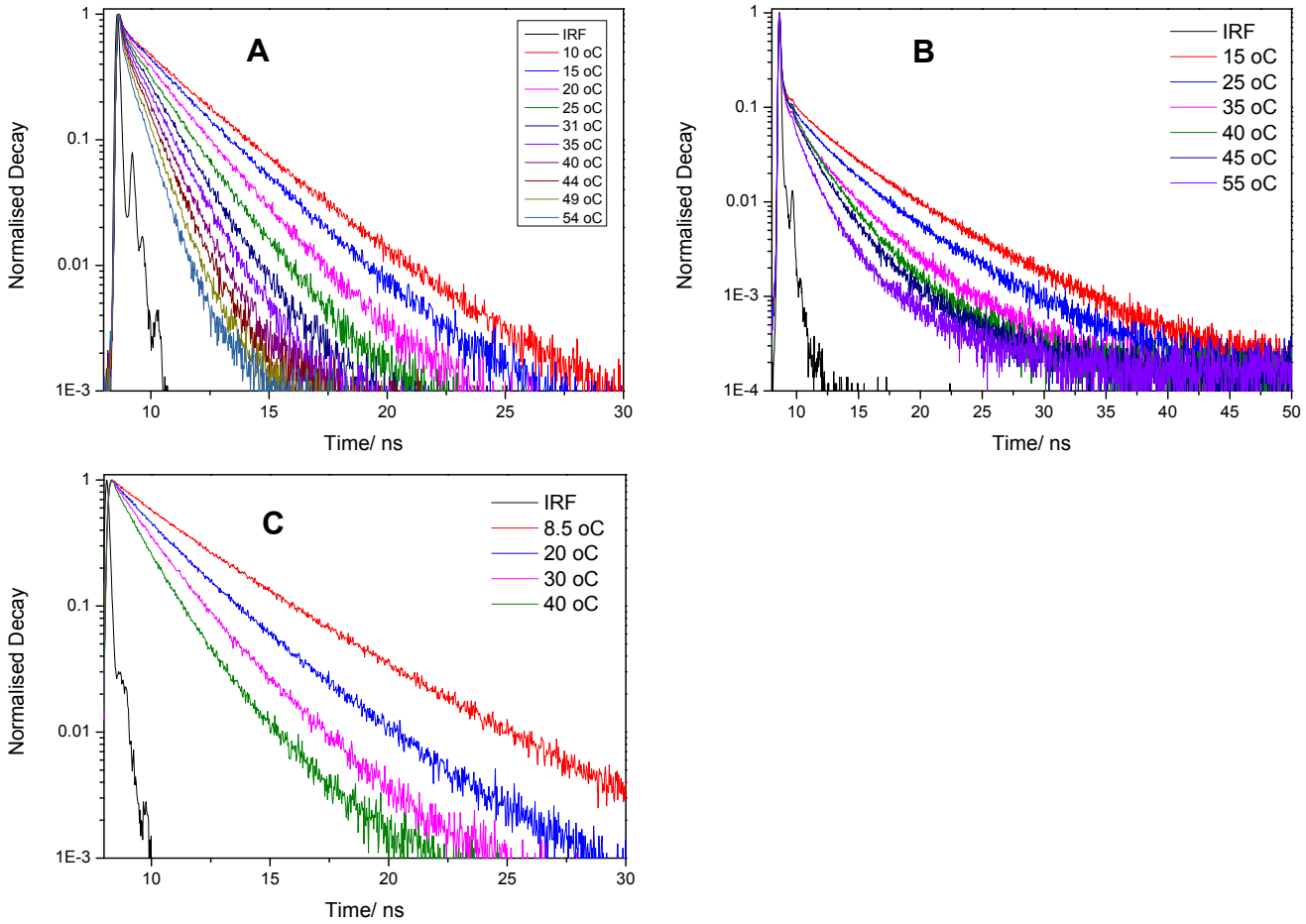

Fig. S8. Time resolved fluorescence decays of **1c** in LUVs of (A) DOPC, (B) EYSM and (C) DOPC:cholesterol 70:30 recorded at various temperatures

Table S1. Fluorescence lifetimes (τ_i) and normalised amplitudes (A_i) obtained from the two- or three-exponential analysis (numerical convolution with IRF) of fluorescence time profiles recorded in model lipid bilayers incorporating **1c** (1:200 [dye]:[lipid)] with compositions DOPC, EYSM, DOPC:cholesterol 70:30 and EYSM:cholesterol 70:30 at various temperatures. The time resolved fluorescence decays are given in Fig. S8 and 1C (main text).

Composition	Temperature, °C	τ_1 / ns	τ_2 / ns	τ_3 / ns	A_1 / %	A_2 / %	A_3 / %
DOPC	10	0.21	2.79	–	10.0	90.0	–
	15	0.20	2.38	–	11.4	88.6	–
	20	0.20	1.98	–	14.1	85.9	–
	25	0.19	1.66	–	16.8	83.2	–
	31	0.16	1.37	–	19.1	80.9	–
	35	0.15	1.22	–	22.4	77.6	–
	40	0.15	1.06	–	25.9	74.1	–
	44	0.14	0.94	–	29.3	70.7	–
	49	0.13	0.85	–	34.4	65.6	–
	54	0.12	0.75	–	40.4	59.6	–
EYSM	15	2.15	6.05	< 0.03	23.6	39.0	37.4
	25	1.85	5.38	< 0.03	25.8	31.9	42.4
	35	1.54	4.54	< 0.03	25.3	22.0	52.7
	40	1.37	3.91	< 0.03	31.5	17.1	51.4
	45	1.17	3.35	< 0.03	28.9	16.8	54.3
	55	0.98	3.23	< 0.03	27.8	10.6	61.6
DOPC:cholesterol 70:30	8.5	1.61	4.04	–	22.9	77.1	
	20	1.08	2.96	–	28.6	71.4	
	30	0.66	2.02	–	24.7	75.3	
	40	0.79	2.09	–	55.5	44.5	
EYSM:cholesterol 70:30	8.5	1.16	5.48	–	25.7	74.3	–
	20	1.01	5.13	–	31.8	68.2	–
	30	0.82	4.60	–	33.9	66.1	–
	40	0.61	3.66	–	35.7	64.3	–

Table S2. The parameters of the biexponential fit of FLIM data obtained with **1c** in several slices of different porcine lenses at 20 °C. Peak maxima and full width of the half maximum (FWHM) of histograms are given.

Lens	Slice	τ_1 / ns		τ_2 / ns		A_1 / %		A_2 / %	
		Peak	FWHM	Peak	FWHM	Peak	FWHM	Peak	FWHM
#1	a	1.07	0.30	4.96	0.45	45.1	6.2	54.9	6.5
	b	0.98	0.24	5.22	0.36	44.8	5.1	55.2	5.3
	c	0.97	0.20	5.21	0.31	46.1	4.6	53.9	4.4
#2	a	1.21	0.37	5.29	0.35	49.1	5.4	50.9	6.5
	b	1.15	0.31	5.41	0.36	48.8	6.0	51.2	6.1
	c	1.12	0.33	5.40	0.41	49.0	5.7	51.0	5.9
	d	1.05	0.29	5.16	0.32	49.5	5.9	50.5	5.6
	e	1.15	0.29	5.20	0.40	48.0	6.0	52.0	5.7
#3	a	1.02	0.25	5.03	0.38	51.2	4.6	48.8	4.5
	b	1.05	0.26	5.07	0.42	49.8	4.8	50.2	4.7
	c	1.06	0.31	4.96	0.45	52.3	5.3	47.7	5.2
	d	1.00	0.22	5.03	0.30	45.9	4.3	54.1	4.8
	e	0.95	0.23	5.18	0.28	45.2	5.1	54.8	5.3
Total		**1.06±0.08**	**0.28±0.05**	**5.16±0.15**	**0.37±0.06**	**48.0±2.4**	**5.3±0.6**	**52.0±2.4**	**5.4±0.7**

Table S3. The parameters of the biexponential fit of FLIM data obtained with **1c** in several slices of a single porcine lens (#1) at 8 and 37 °C. Peak maxima and FWHM of histograms are given.

Temperature	Slice	τ_1 / ns		τ_2 / ns		A_1 / %		A_2 / %	
		Peak	FWHM	Peak	FWHM	Peak	FWHM	Peak	FWHM
8 °C	a	0.96	0.22	5.46	0.37	41.1	5.7	58.9	6.3
	b	1.01	0.24	5.47	0.33	40.0	5.1	60.0	5.7
	c	1.01	0.22	5.48	0.30	40.8	4.5	59.2	5.1
	Total	**0.99±0.03**	**0.22±0.01**	**5.47±0.01**	**0.33±0.04**	**40.7±0.6**	**5.1±0.6**	**59.3±0.6**	**5.7±0.6**
37 °C	a	0.69	0.13	4.77	0.25	50.1	4.5	49.9	4.6
	b	0.74	0.14	4.58	0.27	48.2	4.2	51.8	4.7
	c	0.79	0.17	4.67	0.35	45.4	5.9	54.6	5.3
	d	0.88	0.18	4.70	0.32	53.7	3.9	46.3	3.6
	e	0.83	0.20	4.67	0.30	51.8	4.4	48.2	4.1
	f	0.79	0.22	4.62	0.31	50.2	3.8	49.8	3.7
	Total	**0.79±0.07**	**0.17±0.03**	**4.67±0.07**	**0.30±0.03**	**49.8±3.1**	**4.5±0.8**	**50.2±3.1**	**4.3±0.7**

Table S4. Peak position and FWHM of fluorescence lifetime τ_2 of **1c** averaged over several eye lens slices (data from Tables S2 and S3) measured at various temperatures and viscosity values according to the calibration plot (Figure 2B of the main text).

Temperature	$<\tau_2>$ / ns	FWHM of $<\tau_2>$ / ns	Viscosity / cP
8 °C	5.47	0.33	3500 +1200/-750
20 °C	5.16	0.37	2150 +750/-570
37 °C	4.69	0.30	1050 +200/-170

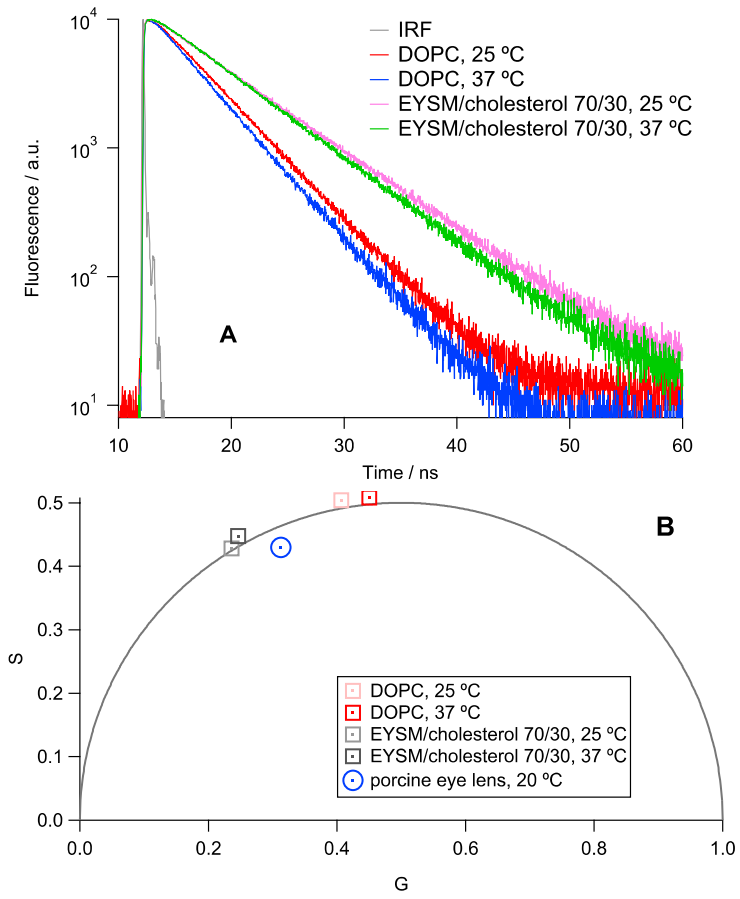

Fig. S9. (A) Time-resolved fluorescence decays recorded for LUVs incorporating di-4-ANEPPDHQ at 1:250 lipid:dye ratio. The data in DOPC and EYSM:cholesterol 70:30 are shown as indicated in the Fig. key, recorded at 25 and 37 °C. (B) Phasor plot of the data presented in (A) together with the FLIM data obtained with porcine eye lens stained with 10 μM PBS solution of di-4-ANEPPDHQ. Two photon excitation was at 860 nm and fluorescence detection was between 440-590 nm. The proximity of the lens data phasor to the model L_o phase phasors indicates the abundance of L_o domains in lens cell membranes.

2. Synthesis and compound characterisation

2.1 General Materials and Methods

The manipulation of all air and/or water sensitive compounds was carried out using standard inert atmosphere techniques. All chemicals were used as received from commercial sources without further purification. Anhydrous solvents were used as received from commercial sources. Analytical thin layer chromatography (TLC) was carried out on Merck® aluminium backed silica gel 60 GF254 plates and visualisation when required was achieved using UV light or I_2. Flash column chromatography was performed on silica gel 60 GF254 using a positive pressure of nitrogen with the indicated solvent system. Where mixtures of solvents were used, ratios are reported by volume. Nuclear magnetic resonance spectra were recorded on 400 MHz spectrometers at ambient probe temperature. Chemical shifts for ^{1}H NMR spectra are recorded in parts per million from tetramethylsilane with the solvent resonance as the internal standard (methanol: δ = 3.31 ppm). ^{13}C NMR spectra were recorded with complete proton decoupling. Chemical shifts are reported in parts per million from tetramethylsilane with the solvent resonance as the internal standard ($^{13}CD_3OD$: 49.00 ppm). ^{19}F NMR spectra were recorded with complete proton decoupling. Chemical shifts are reported in parts per million referenced to the standard hexafluorobenzene: −164.9 ppm. Mass spectra were carried out using ElectroSpray Ionisation (ESI), and only molecular ions are reported. Elemental microanalysis was carried out with LECO CHNS-932 Analyzer. Analytical HPLC (Agilent 1200 system) was performed with ZORBAX Eclipse XDB-C18 5 μm column (Agilent) using 1 mL/min flow and stepwise gradient at 25 °C.

2.2 Synthetic Procedures

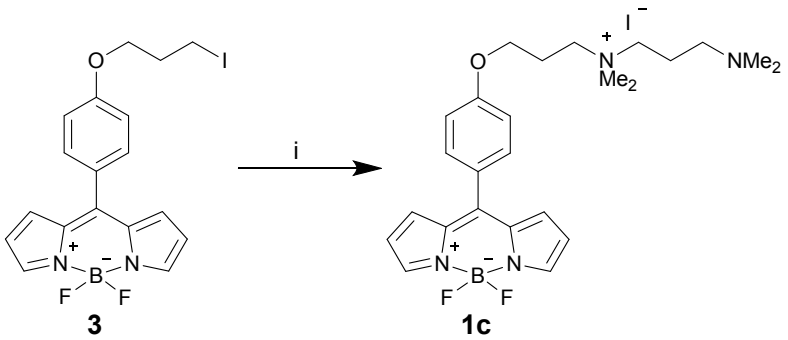

Scheme S1. Synthesis of **BODIPY 1c**: (i) *N*,*N*,*N′*,*N′*-tetramethyl-1,3-propanediamine, tetrahydrofuran (THF), 0 °C to rt, 24h, yield: 83%. **BODIPY 3** was prepared following a reported procedure.[6]

BODIPY 1c. To a cooled solution of **BODIPY 3** (200 mg, 0.44 mmol) in 20 mL of dry THF at 0 °C was added *N,N,N′,N′*-tetramethyl-1,3-propanediamine (10 mL, 60 mmol) under Ar atmosphere. The reaction mixture was stirred at room temperature for 24 h. The resulting dark-red precipitate was filtered, washed with THF (50 mL) and diethyl ether (100 mL) and dried under vacuum to give **BODIPY 1c** as a red-orange solid. Yield: 212 mg (83%).

^{1}H NMR (400 MHz, CD_3OD) δ_H 7.93 (br s, 2H), 7.61 (d, *J* = 8.7 Hz, 2H), 7.19 (d, *J* = 8.7 Hz, 2H), 7.02 (d, *J* = 4.0 Hz, 2H), 6.62 (dd, *J* = 4.0, 1.4 Hz, 2H), 4.26 (t, *J* = 5.5 Hz, 2H), 3.64 (m, 2H), 3.45 (m, 2H), 3.20 (s, 6H), 2.44 (t, *J* = 7.1 Hz, 2H), 2.36 (m, 2H), 2.29 (s, 6H), 1.99 (m, 2H); **^{13}C NMR** (100 MHz, CD_3OD) δ_C 162.65, 148.81, 144.82, 136.07, 133.88, 132.74, 127.86, 119.78, 116.09, 66.21, 63.92, 63.11, 56.90, 51.86, 45.64, 24.12, 21.72; **^{19}F NMR** (377.5 MHz, CD_3OD) δ_F −146.07; **HRMS** (ESI-TOF) m/z 455.2785 ($C_{25}H_{34}BF_2N_4O$, $[M\text{-}I]^+$, requires 455.2788). **Anal. Calcd.** For: $C_{25}H_{34}BF_2N_4OI$: C, 51.57; H, 5.89; N, 9.62, found: C, 51.21; H, 5.71; N, 9.20.

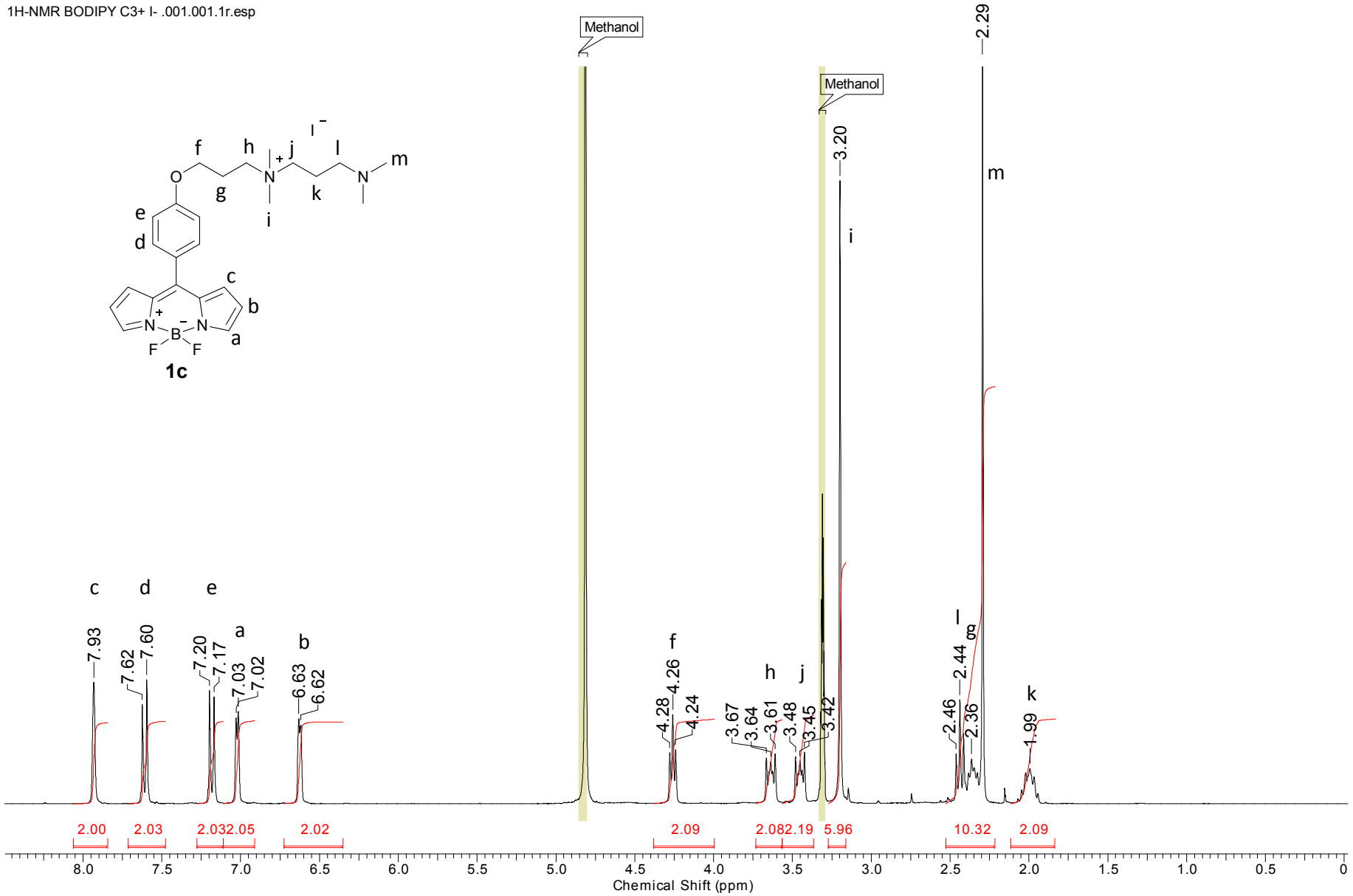

Fig. S10. ^{1}H NMR spectrum of BODIPY **1c** (400 MHz, CD_3OD).

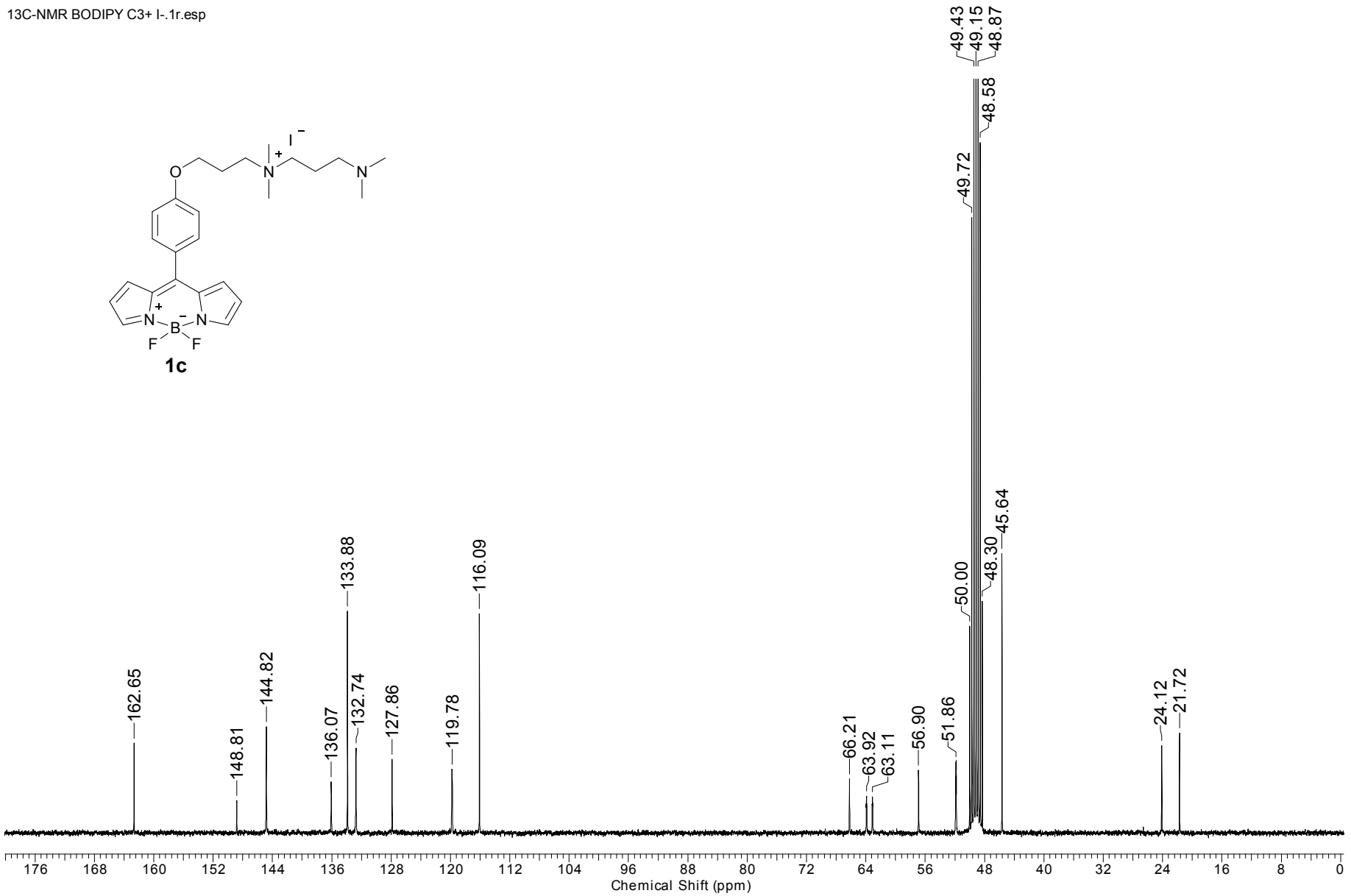

Fig. S11. ^{13}C NMR spectrum of BODIPY **1c** (100 MHz, CD_3OD).

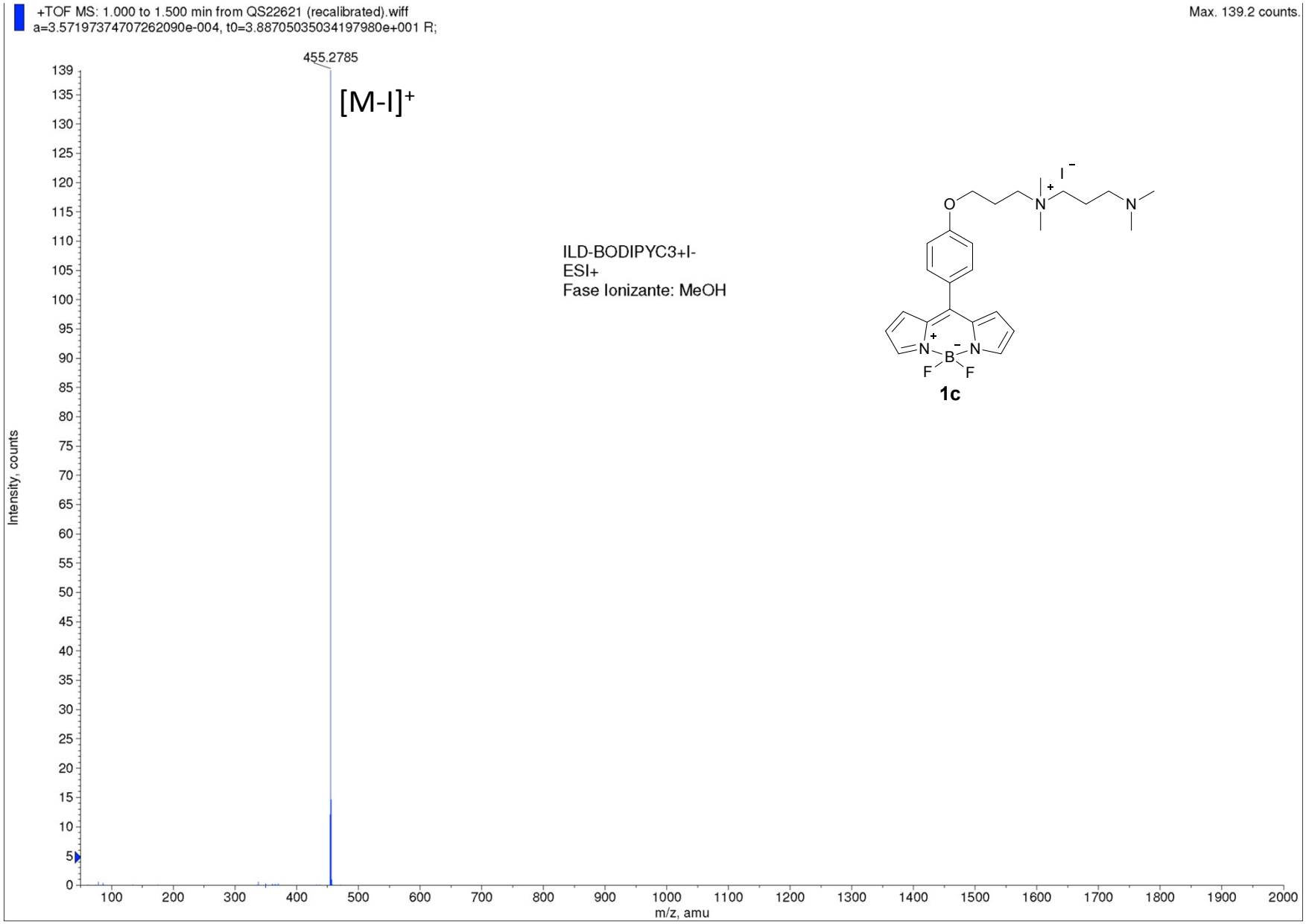

Figure S12. HR MS (ESI+TOF) mass spectrum of BODIPY **1c**.

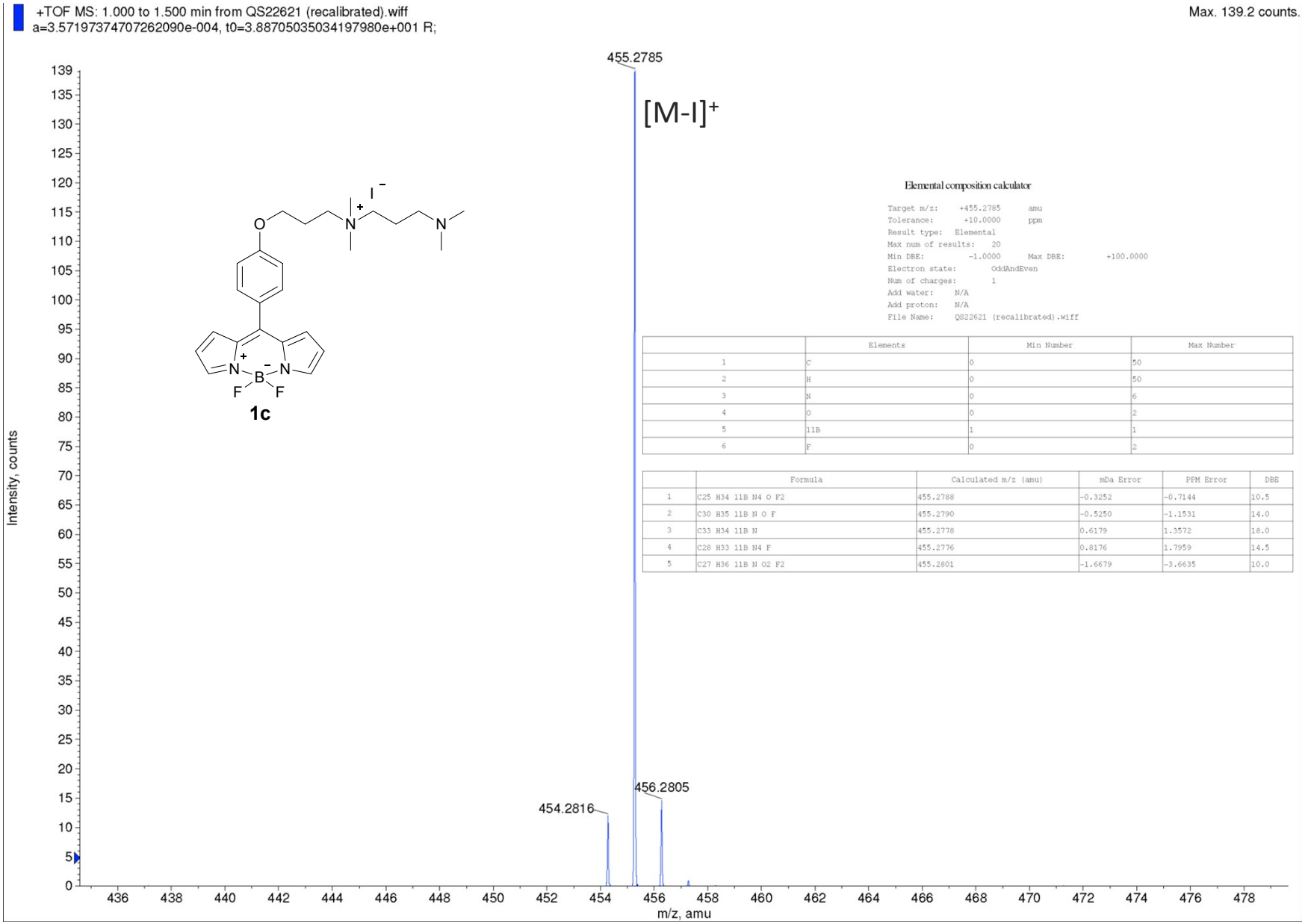

Fig. S13. HR MS (ESI+TOF) mass spectrum of BODIPY **1c**.

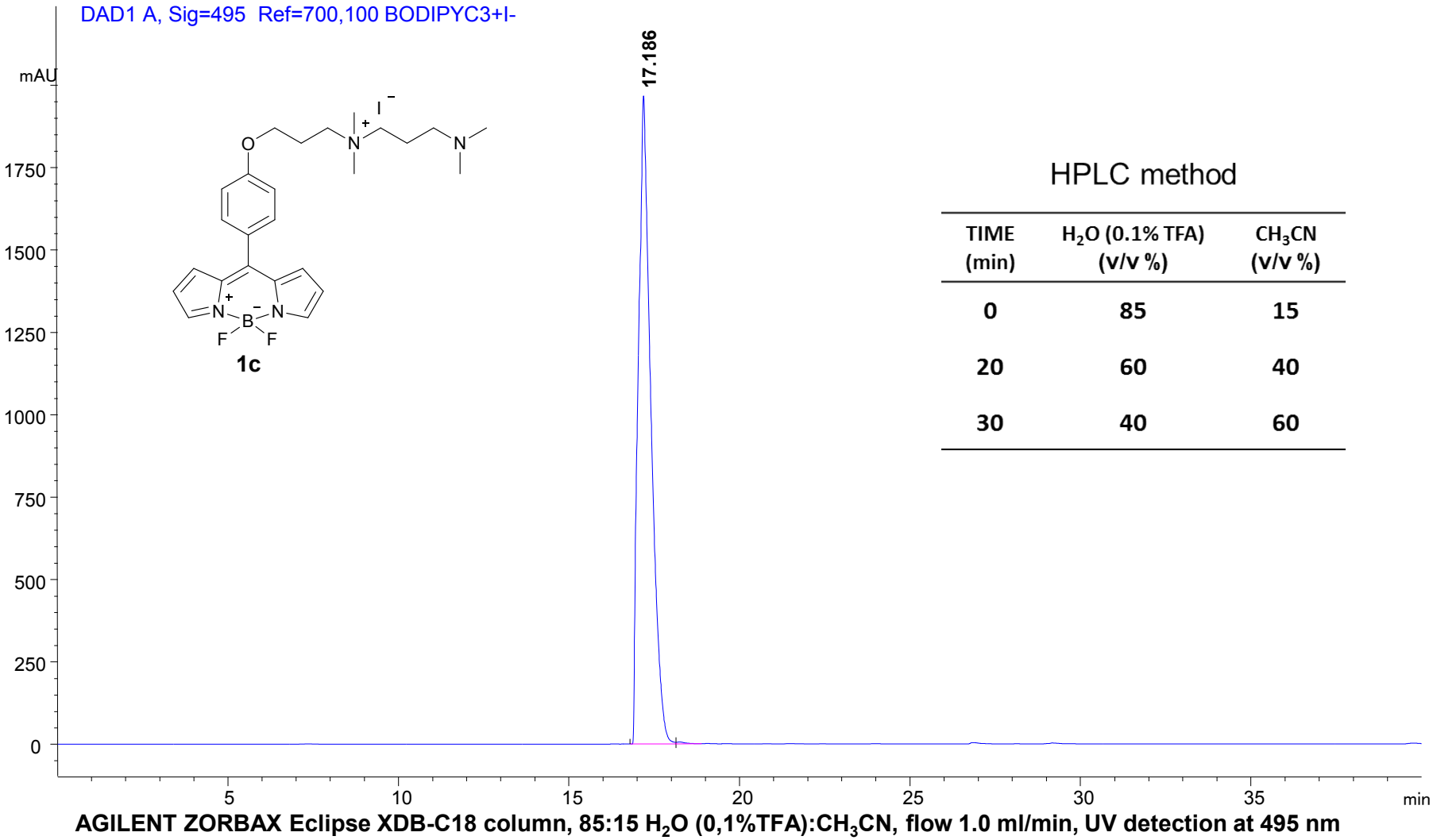

Fig. S14. RP-HPLC trace of BODIPY **1c**. Retention time = 17.186 min.

3. List of references

1. Y. Wu, M. Štefl, A. Olzyńska, M. Hof, G. Yahioglu, P. Yip, D. R. Casey, O. Ces, J. Humpolíčková, M. K. Kuimova, *Phys. Chem. Chem. Phys.* 2013, **15**, 14986.
2. A. Vyšniauskas, M. Qurashi, N. Gallop, M. Balaz, H. L. Anderson, M. K. Kuimova, *Chem. Sci.* 2015, **6**, 5773.
3. M. R. Dent, I. López-Duarte, C. J. Dickson, N. D. Geoghegan, J. M. Cooper, I. R. Gould, R. Krams, J. A. Bull, N. J. Brooks, M. K. Kuimova, *Phys. Chem. Chem. Phys.* 2015, **17**, 18393.
4. I. López-Duarte, T. T. Vu, M. A. Izquierdo, J. A. Bull, M. K. Kuimova, *Chem. Comm.* 2014, **50**, 5282.
5. A. Vyšniauskas, M. Balaz, H. L. Anderson, M. K. Kuimova, *Phys.* Chem. *Chem. Phys.* 2015, **17**, 7548.
6. A. N. Ahmed, E. Gulera, H. I. Ucana, R. W. Boyleb, *Dyes Pigm.* 2012, **94**, 496.